Motion Planning for a Mobile Robot with a Kinematic Constraint

P. Tournassoud and O. Jehl

INRIA, Domaine de Voluceau

BP 105, 78153 Le Chesnay Cedex, France

Abstract

This paper explores the motion planning problem for a mobile robot with a kinematic constraint, this is, the number of its degrees of freedom is less than the dimension of its Configuration Space. Addressing first the "local" problem of turning in a corridor, we show that sliding continuously on the outer wall in a turn constitutes a canonical contact trajectory, in the sense that if it is not safe, there cannot be another safe trajectory with no backing-up maneuver. In the case no smooth trajectory exists, we propose some simple maneuvers.

A heuristic path planning algorithm based on a decomposition of free space into cones connected by turns is then presented. Finally we discuss how this can apply within the more realistic framework of a real mobile robot at work, by implementing these results as a set of rules of behaviour for the robot.

1 Introduction

Path planning for a manipulator robot moving among obstacles is now well understood. This is a difficult problem [SS83], but some practical algorithms have been proposed following the pioneering work of Lozano-Pérez and Wesley [LW79]. The basic idea behind most algorithms is to build a representation of free space in Configuration Space as a connectivity graph of free regions, that can then be searched for a path. The practical limitation due to the complexity of the representation can be alleviated by limiting the number of degrees of freedom taken into account exhaustively [Fav84,Loz86], or by using a mixed local and global approach [FT87a,FT87b].

Motion planning for an object in the plane is easy if it performs only translations, the boundary of free space being simply obtained by growing obstacles to represent sliding motions of the robot on their contours. When rotations are allowed, the explicit computation of configuration obstacle surfaces, if more complex, remains possible [ABF88]. Most algorithms nevertheless rely on a discretization of orientation ranges [LW79,BL85].

Yet very little attention has been devoted so far to the basic issue posed by motion planning for mobile robots : as opposed to manipulator robots, whose bindings between bodies effectively decrease the dimension of their Configuration Space, those are usually subject to kinematic constraints that turn them into non-holonomic systems. Indeed, a mobile robot with two driving wheels mounted on the same axis can only move in the direction normal to the axis, a car can only turn around a point located along the rear axle... Such systems, though their position is described by three-dimensional configuration vectors, have only two degrees of freedom.

Much of our interest in this problem must be credited to Laumond. [Lau86] demonstrates that the existence of a trajectory for a mobile robot is unaffected by the kinematic constraint. [Lau87] addresses more the problem of a lower bounded turning radius than that of the kinematic constraint stated above. Indeed, as it uses a mobile robot of circular symmetry, raising the constraint on the turning radius will make the problem equivalent to planning a path for a disc without any specific constraint. We recall this 2D problem can be solved in a straightforward manner by using a generalized visibility graph (composed of arcs of circles and line segments) built from the obstacles grown by the radius of the disc.

The decomposition used by Brooks [Bro82] is of interest in our context. Free space in the plane is represented by a union of generalized cones, that capture freeways between pairs of facing walls. The motion of the robot is decomposed into pure translations along the spines of the cones, and pure rotations at points where spines intersect. Planning is performed by propagating constraints on the range of legal orientations along a given sequence of cones. No specific orientation is imposed for a translation, so this does not answer the question of path planning with a kinematic constraint. It could be done simply by imposing that the robot is oriented along the axis of the spine during a translation. Yet this would be very restrictive, as not much would be left to be propagated during a search.

In this paper we begin by addressing the more restricted problem of turning in a corridor. We introduce contact trajectories, a refinement of the notion of C-surface in this context : they are defined by the contact of the robot with an obstacle at one point, plus the kinematic constraint. We show that sliding continuously on the outer wall of a turn constitutes a canonical contact trajectory : it is such that if it is not safe, there cannot be another safe trajectory with no backing-up maneuver.

We then describe a heuristic motion planning algorithm, which makes it possible to control the number of maneuvers necessary along a path. It makes use of a decomposition of free space into cones connected by turns : a connectivity graph is built whose arcs represent contact trajectories in turns, and possible links in corridors between them.

Finally we show how these ideas can be incorporated in the more realistic framework of a real mobile robot at work. We choose to implement these results as a set of rules of behaviour for the robot : using a combination of information from on-board sensors and higher level knowledge on its environment, the robot reproduces canonical trajectories without pre-computing them.

2 Kinematics of the Mobile Robot

The mobile robot is a vehicle with two driving wheels mounted on the same axis, controlled independently, plus one free wheel. In the sequel, we assume for simplicity that its body is rectangular, though any polygonal shape would lead to similar results. A configuration vector $\mathbf{q}$ consists in the 3-tuple (x, y, θ), with x and y the coordinates in the plane of point O of the robot at mid-distance from the driving wheels, and θ its orientation. Nevertheless, the robot has only two degrees of freedom : we write $\mathbf{v}$ the vector of components v and v', products of angular velocities of the wheels by their radius (see fig. 1a).

We get the equations of motion :

$$\dot{x} = \cos\theta \, \frac{v + v'}{2}, \quad \dot{y} = \sin\theta \, \frac{v + v'}{2}, \quad \dot{\theta} = \frac{v - v'}{2d}, \tag{1}$$

with d equal to half the distance between the driving wheels. We also write these equations $\dot{\mathbf{q}} = \mathbf{K}(\theta)\mathbf{v}$, as $\mathbf{K}$ depends only on angle θ.

Equations 1 implicitely contain the constraint of non-holonomicity of the vehicle :

$$dy = \tan\theta \; dx \tag{2}$$

It simply states that the robot can only move in the direction normal to the axis of the driving wheels.

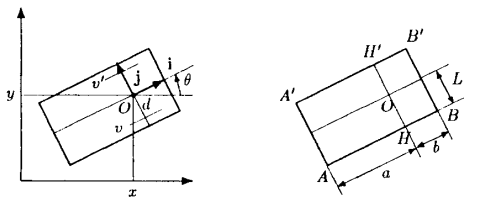

(a) (b)

Figure 1: Kinematics (a) and geometry (b) of the mobile robot.

For a point $\mathbf{m}$ bound to the robot with coordinates (p, q) in its relative frame $(O, \mathbf{i}, \mathbf{j})$ (as represented on fig. 1a), we get :

$$\dot{\mathbf{m}} = \mathbf{L}(\theta)\dot{\mathbf{q}} = \begin{pmatrix} 1 & 0 & -p\sin\theta - q\cos\theta \\ 0 & 1 & p\cos\theta - q\sin\theta \end{pmatrix} \dot{\mathbf{q}} \qquad (3)$$

Writing the standard differential relation $\dot{\mathbf{m}} = \mathbf{J}\,\mathbf{v}$, where $\mathbf{J}$ is the jacobian matrix at point $\mathbf{m}$ for configuration $\mathbf{q}$, we derive from equations 1 and 3 that :

$$\mathbf{J} = \frac{1}{2}\begin{pmatrix} \cos\theta & \cos\theta \\ \sin\theta & \sin\theta \end{pmatrix} + \frac{1}{2d}\begin{pmatrix} -p\sin\theta - q\cos\theta & p\sin\theta + q\cos\theta \\ p\cos\theta - q\sin\theta & -p\cos\theta + q\sin\theta \end{pmatrix} \qquad (4)$$

A trajectory of the robot is a curve in 3D-space :

$$t \rightsquigarrow \Gamma(t) = \mathbf{q}_0 + \int_{t_0}^{t} \mathbf{K}(\theta)\mathbf{v}\; dt$$

For a point bound to the robot it yields a trajectory in the plane :

$$t \rightsquigarrow \gamma(t) = \mathbf{m}_0 + \int_{t_0}^{t} \mathbf{J}(\theta)\mathbf{v}\; dt$$

In the sequel γ will denote the trajectory traced by point O of the robot. The radius of curvature of γ is equal to :

$$\rho = d\,\frac{v + v'}{v - v'} \qquad (5)$$

Hence a cusp point of γ either corresponds to a turn on the spot $(v = -v' \neq 0)$, or a backing-up maneuver $(v = v' = 0)$. As far as path planning is concerned, the only significant cusp points of the trajectory are backing-up maneuvers : indeed, a turn on the spot can always be regularized so as to yield a smooth trajectory for which the surface swept by the robot is as near from the original than we wish. Until section 5, we will impose that the trajectory γ of point O be smooth unless at finitely many cusp points that we know correspond to backing-up maneuvers.

Proposition 1 *From the trajectory γ of point O, we can derive the trajectory Γ of the robot in its Configuration Space.*

Proof: From the parametrization $t \rightsquigarrow s(t) = \int_{t_0}^{t} \sqrt{\dot{x}^2 + \dot{y}^2}\; dt$ of trajectory γ we derive $v + v'$. From its radius of curvature we derive the ratio v'/v (see eq. 5). □

The proposition below, from Laumond [Lau86], states that the *existence* of a safe trajectory for the mobile robot between an initial and a goal configuration is unaffected by the kinematic constraint.

Proposition 2 (Laumond) *Between two safe configurations that belong to the same connected component of free space, there exists a trajectory that respects the kinematic constraint.*

It follows from compactness of the space swept by the robot along a trajectory of finite length. Though constructive, the proof given in [Lau86] is of little practical interest : indeed, if we try to deduce a trajectory respecting the kinematic constraint from an arbitrary trajectory in Configuration Space, it is difficult to control the number of maneuvers necessary along a path.

3 Turning in a Corridor

We first concentrate on a more restricted problem, that of making a turn in a corridor, described by two walls, each one with an angular point. These are the "outer" obstacle S_e and "inner" obstacle S_i of figure 2. We assume S_i and S_e^c are convex (S^c denotes the complementary of a set S). Say the robot comes from the left. In the sequel, edge e^- will stand for the first edge of obstacle S_e, e^+ for the latter one.

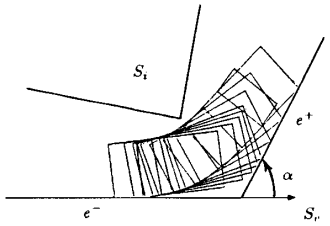

Figure 2: Description of the corridor and canonical contact trajectory.

This can be considered as a "local" motion planning problem, that we will in section 6 incorporate in a global planning scheme (for instance, the algorithm of Brooks [Bro82] uses a similar decomposition). In the absence of any kinematic constraint, that problem is simple. In the case we want to move a rectangular object through the corridor, we would simply check (with notations of fig. 1b) whether when moving with point A sliding on edge e^- of external wall S_e, point B on e^+, the surface swept by the robot intersects the inner wall S_i or not. Recall that for such trajectories defined by a double vertex-edge contact between the moving object and the obstacles, points bound to the robot follow ellipses in the plane, and the enveloppe of segment $A'B'$ is an astroid. As we now deal with a system incorporating a kinematic constraint, it is natural to study trajectories that remain *at one point* in contact with an obstacle, the remaining degree of freedom being determined by the kinematic constraint. This refines the notion of C-surface in this context.

In the case of a rectangular shaped body, contact motions can be of the following types. The case when a vertex of the robot remains in contact with an edge of an obstacle (see fig. 3a) will be examined in detail in the next section. In the case of a contact between edges AB or $A'B'$ of the robot and a vertex of an obstacle, the robot can only move in a straight line, unless contact occurs at points H or H' (points on the axis of rotation of the driving wheels), in which case it can turn on the spot around this point (fig. 3b,c). A last case is the contact between edges AA' or BB' of the robot and a vertex of the obstacles, as discussed in section 5 (fig. 3d).

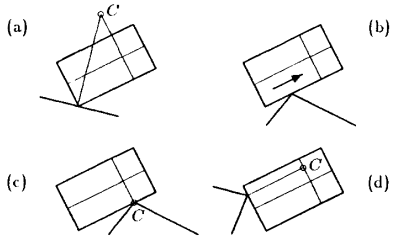

Figure 3: Possible contact motions (point C is the center of rotation).

4 Sliding along the outer wall

We now explicitely write the equations of motion for the robot sliding on the outer wall. The parameters for the geometry of the robot are

those of figure 1b : $a = \|HA\|$, $b = \|HB\|$, L is the half-width of the robot. To make the equations simpler, we align x-axis with edge e^-.

Let us assume the robot slides on the outer wall before the turn (horizontal edge e^- of figure 2), remaining in contact with point A. We get easily :

$$y(\theta) = a\sin\theta + L\cos\theta \tag{6}$$

From that equation and the kinematic constraint (eq. 2), we derive :

$$x - x_0 + a(\cos\theta + \ln|\tan\frac{\theta}{2}|) - L\sin\theta \tag{7}$$

The radius of curvature for the trajectory γ of point O equals :

$$\rho = \frac{a}{\tan\theta} - L \tag{8}$$

so there exists a cusp point on γ for $\tilde{\theta} = \arctan(a/L)$.

Let us call α the angle between edges e^- and e^+ of outer wall S_o (fig. 2). In this section, we will suppose that $\alpha \leq \pi/2$. If we want the mobile robot to slide continuously along edge e^-, then e^+, the double contact configuration must be such that normals to the edges at contact points intersect along the axis of the driving wheels (see fig. 4).

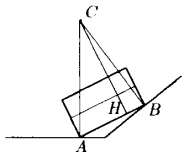

Figure 4: The double contact configuration.

The corresponding orientation $\theta^\star$ thus verifies :

$$\rho = \frac{a}{\tan\theta^\star} - L = \frac{b}{\tan(\alpha - \theta^\star)} - L \tag{9}$$

This is, we get $\tan(\alpha - \theta^\star) = b/a\ \tan\theta^\star$, or :

$$\theta^\star = \frac{1}{2}(\alpha + \arcsin(\frac{a-b}{a+b}\sin\alpha)) \tag{10}$$

We also derive the corresponding value for x_0 in equation 7, with the origin of the x axis at the vertex of S_o :

$$x_0 = \frac{a+b}{\tan\alpha}\sin\theta^\star - b\cos\theta^\star - a\ln|\tan\frac{\theta^\star}{2}| + L\sin\theta^\star \tag{11}$$

If we slightly translate that trajectory to the right, then the robot necessarily collides with edge e^+ of obstacle S_i. If we translate it to the left, the robot never touches that edge*. We call $\gamma^\star$ the trajectory we obtain by pasting the two pieces together, as illustrated on figure 2. Note that in the case $L < \sqrt{ab}$, that is, a robot that is not "larger than long", trajectory $\gamma^\star$ remains smooth, as $\theta^\star < \tilde{\theta}$ (and the converse for the second part of the trajectory is equally true). In the sequel, we will assume for clarity that this condition is verified, though it does not introduce major changes in the following results.

We will note $R(\gamma)$ the surface swept by the body of the robot when it describes trajectory γ. We say a trajectory γ for which $R(\gamma)$ does not intersect the obstacles is *safe*. The following proposition characterizes the corridors in which the robot does not need to maneuver.

Proposition 3 *There exists a safe trajectory with no backing-up maneuver only if $\gamma^\star$ is safe.*

Proof: It proceeds in two steps. First, from a smooth and safe trajectory γ, we will derive another smooth admissible trajectory that is convex (θ keeps increasing along the trajectory) (1). Then we will show that γ' can only be "above" $\gamma^\star$, so that $\gamma^\star$ does not intersect the inner wall (2), which will complete the proof.

(1) Let γ be a smooth safe trajectory as illustrated by figure 5. Then let γ' be the boundary of the union of half-planes below γ that do not intersect γ, and whose bounding lines have an orientation lying in between 0 and α. γ' is composed of a finite alterning sequence of arcs of γ and of line segments, with equal tangents at common end-points.

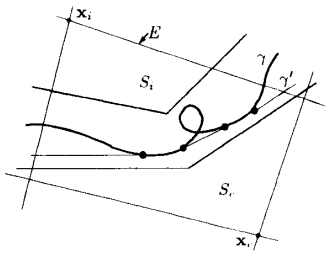

Figure 5: Construction of a convex trajectory.

It is easily seen that $R(\gamma')$ does not intersect the outer wall. This is obvious at points $\mathbf{m}$ of $\gamma \cap \gamma'$. Other points of γ' lie on segments $[\mathbf{m}^-, \mathbf{m}^+]$, with both $\mathbf{m}^-$ and $\mathbf{m}^+$ on $\gamma \cap \gamma'$. The conclusion follows by convexity of S_o.

We now show that $R(\gamma')$ does not intersect the inner wall. First, for a set S that cuts free space F inside the corridor in two connected components, we define $Sup(S)$ as the connected component of $F \setminus S$ "above" S †.

Let $\oplus$ denote the Minkowski sum, and D_L a disc of radius L. We will need the following lemma.

Lemma 1 *For any convex trajectory γ' :*

$$Sup(R(\gamma')) = Sup(\gamma' \oplus D_L)$$

This follows from the fact that the trajectory of point H' of the robot is tangent to its body at that point. Note that even in the case the trajectory of point H' has cusp points, the lemma holds.

Lemma 2 *For any trajectory γ :*

$$Sup(\gamma \oplus D_L) = (Sup(\gamma)^c \oplus D_L)^c$$

Lemma 3 *Let γ designate any smooth trajectory. We denote $\gamma \oplus^\perp S_L$ the union for $\mathbf{m} \in \gamma$ of points $\mathbf{m} + \xi\mathbf{n}$, with $\mathbf{n}$ the unit vector normal to γ at point $\mathbf{m}$ and $\xi \in [-L, L]$. Then :*

$$Sup(\gamma \oplus D_L) = Sup(\gamma \oplus^\perp S_L)$$

We derive that :

$$\begin{aligned}
Sup R(\gamma') &= Sup(\gamma' \oplus D_L) && \text{by lemma 1} \\
&= (Sup(\gamma')^c \oplus D_L)^c && \text{by lemma 2} \\
&\supset (Sup(\gamma)^c \oplus D_L)^c && \text{as } Sup(\gamma') \supset \gamma \\
&= Sup(\gamma \oplus D_L) \\
&= Sup(\gamma \oplus^\perp S_L) && \text{by lemma 3} \\
&\supset Sup(R(\gamma)) && \text{as } R(\gamma) \supset \gamma \oplus^\perp S_L \\
&\supset S_i
\end{aligned}$$

This ends the first part of the proof.

(2) It remains to be shown that γ' necessarily lies "above" $\gamma^\star$, this is $Sup(\gamma^\star) \supset \gamma'$. Then equations very similar to those above show that $\gamma^\star$ does not intersect the inner wall, which completes the proof.

*A nice consequence of equation 8 is that the trajectory of point H, and a fortiori that of B, has no cusp point and is convex.

†For this to be done rigorously, we consider two points $\mathbf{x}_i$ and $\mathbf{x}_o$ far inside obstacles S_i and S_o respectively. We call E the bounded portion of the plane as delimited on figure 5. For any set S such that $\mathbf{x}_i$ and $\mathbf{x}_o$ belong to two distinct connected components of $E \setminus S$, we define $Sup(S)$ as being the connected component of $E \setminus S$ containing $\mathbf{x}_i$.

Let us assume the contrary. We call $\mathbf{m}^-$ and $\mathbf{m}^+$ two consecutive intersection points of γ and γ' such that in between γ' lies below γ^*.
• First suppose that at $\mathbf{m}^-$ and $\mathbf{m}^+$, the contact of the robot for trajectory γ^* occurs with the same edge of S_c, say edge e^-. Then at $\mathbf{m}^+$, $\theta^+_{|\gamma'} < \theta^+_{|\gamma^*}$, and the robot intersects the outer wall at $\mathbf{m}^+$ for γ', which is wrong.
• If for γ^* the robot is at $\mathbf{m}^-$ in contact with edge e^- of S_c, at $\mathbf{m}^+$ with edge e^+, then :
- at $\mathbf{m}^-$ $\theta^-_{|\gamma'} < \theta^-_{|\gamma^*}$,
- at $\mathbf{m}^+$ $\theta^+_{|\gamma'} > \theta^+_{|\gamma^*}$.
The point $\mathbf{m}^*$ of double contact with the outer wall for γ^* lies in between $\mathbf{m}^-$ and $\mathbf{m}^+$. Then there exists on γ' a point $\mathbf{m}'$ located between $\mathbf{m}^-$ and $\mathbf{m}^+$, such that $\theta' = \theta^*$. As $\mathbf{m}'$ lies below the line tangent to γ^* at $\mathbf{m}^*$, it contradicts the fact that at $\mathbf{m}'$ the robot does not intersect the outer wall. □

We have thus proved the existence of a canonical motion that remains in contact with the outer wall : it is such that if we want to verify the existence of a trajectory without maneuver, we only have to check that for this particular motion the robot does not intersect the inner wall. This is done by simply testing whether the trajectory traced by point H' of the robot stays below that wall.

5 More information when the contact trajectory γ^* is not safe

We introduce another class of canonical trajectories of interest, defined by the possible simultaneous contacts of the robot with the inner and outer walls. γ^- is the trajectory obtained by sliding on edge e^- of S_c while coming in contact with inner obstacle S_i. Two cases can happen. Either the contact occurs between the vertex of S_i and point H' of the robot (fig. 6a), or between the latter edge of S_i and point B'. In fact, another eventuality is that for all possible sliding motions of the robot on edge e^-, no contact with S_i ever occurs (in which case, easy strategies exist for turning in the corridor). Symmetrically, we can define γ^+ as the motion obtained by sliding on edge e^+ of S_c with point B and coming in contact with S_i (fig. 6b). We define θ^- and θ^+ to be the orientations of the robot for the two point contact configurations when they exist, on γ^- and γ^+ respectively. Necessarily, $\theta^+ < \theta^-$.

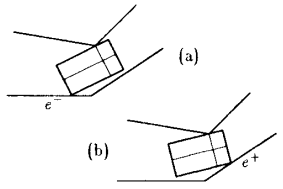

Figure 6: Simultaneous contacts with the inner and outer walls.

We will now suppose γ^* is not safe, but that there exist safe paths with maneuvers. Recall this is checked by verifying that the enveloppe of segment $A'B'$ for the double contact sliding motion on S_c stays below S_i (section 3).

Proposition 4 *Suppose there exist some safe paths, but γ^* is not safe (or equivalently, there exists no safe path without maneuver). Then one of the inequalities $\theta^* < \theta^+$ or $\theta^- < \theta^*$ holds. For the double contact configuration that realizes the inequality, contact with the inner wall is at point H'.*

Proof: $R(\gamma^*)$ intersects S_i. Translate γ^* along edge e^- to the right until $R(\gamma^*)$ is tangent with S_i (at point H'). Indeed, this can always be done, as the minimum distance between S_i and S_c must be more than the width of the robot $2L$. Otherwise, there clearly is no safe path through the corridor, even including maneuvers. Let θ_x be the orientation of the robot at the double contact configuration. Symmetrically, translate γ^* along edge e^+ towards the bottom until $R(\gamma^*)$ is tangent with S_i. Call θ_y the orientation at the double contact configuration. It is easy to check that $\theta_x < \theta_y$. Then at least one of the following inequalities is true, $\theta_x < \theta^*$ or $\theta^* < \theta_y$. If, for instance, $\theta_x < \theta^*$ holds, then necessarily the configuration corresponding to θ_x is on γ^-, θ_x equals θ^-, and this is a double contact configuration. Contact with S_i occurs at point H'. □

For the rest of this section, we concentrate on trajectory γ^- and suppose that $\theta^- < \theta^*$. If this is not the case, similar results can be derived using γ^+.

Proposition 5 *Again suppose there exist some safe paths, but only with maneuvers. Call θ' the orientation of the robot when it collides with edge e^+ of S_i on trajectory γ^-. Then with $\theta^- < \theta^*$, necessarily $\theta^- < \theta' < \theta^*$.*

Proof: Suppose this is not true, then $\theta' < \theta^- < \theta^*$. Now imagine we widen the corridor by translating edge e^+ to the right in the direction of e^-. While we push the wall θ' keeps increasing (it would ultimately reach θ^*). On the way we necessarily find a position of wall e^+ for which $\theta' = \theta^-$, this is, a three point contact. For this enlarged corridor, there thus exists no safe trajectory for the robot. Moreover, this is true of the original problem. □

We can then assume that the robot touches the inner wall before colliding with edge e^+. In that case, we propose the following sequence of simple maneuvers, starting at the two point contact configuration on γ^-. An element of the sequence is composed of :
• *a move in straight line until point B touches edge e^+,*
• *then a rotation around H anti-clockwise until point A comes into contact with edge e^- (this is a backing-up maneuver).*

We can check that no other contact can occur during those moves. As we repeat them, either the orientation of the robot converges towards some angle less than α, and it is blocked, or we reach an orientation superior to α and the turn can be completed. In practice, we would limit ourselves to testing a small number of iterations and declare we found no path if the orientation of the robot is still less than α.

Remark: *What to do in a corridor with a sharp turn ?*

Even in the case $\alpha > \pi/2$, we can exhibit a trajectory for which the robot slides continuously on edge e^-, then e^+. In case the turn is very sharp, this can necessitate sliding with point A' of the robot in contact with e^- after sliding with point A. What has been stated above holds with little modification, the main difference being that the contact trajectory can incorporate two backing-up maneuvers.

In a sharp turn, another class of interesting trajectories is obtained by sliding on the vertex of inner obstacle S_i with edge AA' in contact, as illustrated on figure 7a. This implies one backing-up maneuver, and the robot keeps moving backwards after the turn is completed.

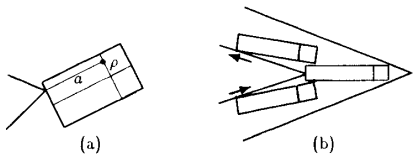

Figure 7: Backing-up maneuver in a corridor with a sharp turn.

We recall ρ is the radius of curvature for point O of the robot. The differential equation of this particular contact motion writes :

$$d\rho = a\, d\theta \tag{12}$$

We derive the equations of motion, with ξ and χ the coordinates of the vertex of obstacle S_i in an absolute frame :

$$x = \xi + a\cos\theta + a(\theta - \theta_0)\sin\theta \tag{13}$$

$$y = \chi + a\sin\theta - a(\theta - \theta_0)\cos\theta \tag{14}$$

Equation 12 implies that the change of orientation after the contact motion is completed equals $\Delta\theta = 2L/a$. Indeed, if the angle between the two edges of S_i is less than $\Delta\theta$, then a complete motion would include :

- *sliding on the first edge of S_i with point A' in contact,*
- *maneuvering keeping edge AA' in contact with the vertex of S_i,*
- *and finally sliding on the latter edge of S_i with point A in contact.*

This is illustrated by the example of figure 7b. A furniture remover has to move a long and heavy sofa in a narrow corridor with a sharp turn. Then he would place wheels at the very front of the sofa, stay at the back and slide along the inner wall, moving backwards after the turn.

6 A planner for a mobile robot with a kinematic constraint

We build a model of the corridors in which the robot can navigate from a planar map of the environment in the following manner. We first construct the Voronoi diagram of the obstacles, represented by polygons, and call *cone* the two linear constraints representing two facing walls at mid-distance from a line segment of the Voronoi diagram. The adjacency of two cones can be easily determined by checking that at least two of the corresponding segments share a common end-point, or that one segment is common to both cones. Our model of free space is thus simply composed of pairs of adjacent cones, each pair defining a turn as studied above.

We are aware of two difficulties arising when using this simple decomposition technique. First of all, a turn can be obstructed by other obstacles, in which case we must redefine two smaller corridors free of any obstacle. Secondly at star-shaped intersections, we can miss legal paths simply because we constrain paths to stay within a sequence of cones. Nevertheless the decomposition we obtain is quite straightforward for most indoor environments. Note that some very simple pre-processing can be done, such as eliminating cones whose minimum clearance (computed on the edges of the Voronoi diagram) is less than the width $2L$ of the robot.

We then build a connectivity graph representing paths of the robot along the corridors. Nodes of the graph stand for cuts perpendicular to the spines of cones, located just before and after a turn (see fig. 8). The cut before the turn, for instance, must be placed such that when rotating with point O on the cut, the robot can only come into contact with edges of S_i and S_j located before the turn. Recall the robot can turn on the spot, so that the height of point O on the cut provides all relevant information.

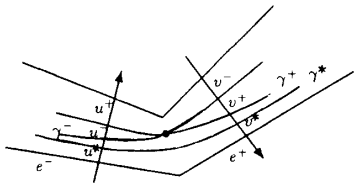

Figure 8: A turn, cuts and reference paths.

Transitions in the graph are of two types. The first class of transitions represent trajectories between two cuts in a turn. The latter stands for paths of the robot within a cone, connecting a cut at the exit of a turn with the entry cut of the next turn.

The graph can embody different levels of sophistication. Say first that we are only interested in paths with no backing-up maneuver. Then there will be no transition in turns whose γ^* trajectories intersect the inner wall. Other cuts will be typically split into three nodes, representing entry or exit points of γ^*, γ^- and γ^+ trajectories. As illustrated on figure 8, let u^*, u^-, u^+ represent the corresponding points on the entry cut of the turn, and v^-, v^+, v^* points on the exit cut. We make use of the four transitions :

$$u^* \mapsto v^*, u^- \mapsto v^-, u^+ \mapsto v^+, u^+ \mapsto v^-. \tag{15}$$

The first three transitions are executed by staying on the corresponding canonical trajectories. The last one decomposes into a sliding motion on e^+, a turn on the spot around the vertex of S_i, and finally a sliding motion on e^-. The asumption behind this limited choice of transition trajectories is that they represent well the propagation of constraints in a sequence of turns[‡]. For instance, it is better to stay on the right in a sequence of left turns, it is preferable to be on the leftmost trajectory in a left turn preceding a turn to the right, etc.

There will exist a transition between two nodes at each end of a cone if we can connect them using a trajectory with no maneuver. Note that this is always true if the corridor is long enough. Otherwise, this is easy to check. The only difficulty arises when the robot has got to slide on one wall at an end of the cone, on the opposite one at the other. Then we simply verify that the two curves we obtain (of the type of equation 7) can be smoothly connected (fig. 9a). Otherwise (fig. 9b), some maneuvers are needed.

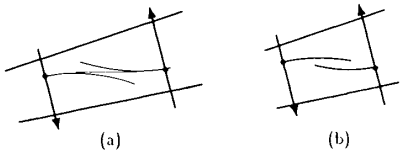

Figure 9: Checking a transition inside a cone.

A more complicated version could incorporate sequences of maneuvers as described in section 5. Note that in this last case, the robot can be moving tail first after the turn. We must be aware that a turn is indeed described by two sets of nodes as described above, depending whether the robot comes head or tail first. Corridors that are large enough can then be used for intra-cone connections that necessitate U-turns. Planning is performed using a cost function combining the length of a path and a special penalty when maneuvering is necessary.

7 Implementing these results as rules of behaviour

We now describe our practical implementation of these results for the navigation of a mobile robot. Its essential features is that it relies more on information from sensors than on pre-defined planning, though it incorporates some features of global planning as described in the previous section. The robot can operate under two distinct modes.

In the first mode, the robot has no knowledge of its environment, except what it learns by reading the measures of its ultrasonic sensors. When a goal configuration is given to it, a free mode trajectory is first computed among those linking the origin and the goal with two arcs of circles. It is chosen so that it minimizes a compromise between the length of trajectory γ of point O, and the discontinuity of its radius of curvature when we switch from one circular arc to the other. The robot will eventually be deviated by obstacles on the way as explained below, so the whole computation of a free mode trajectory and constrained trajectory needs to be performed at each time increment. Deviating the robot is performed by applying very simple rules such that :

- If the robot sees an obstacle in front of him, he tries to move parallel to it, even forgetting temporarily his goal if necessary.
- If the back of the robot is very close to a wall and he wants to move away, then the best he can do is slide along the wall with nearest point

[‡]If the γ^- and/or γ^+ trajectories do not exist because there is no corresponding double contact configuration (the corridor is too wide), transition trajectories with the same characteristics can nevertheless easily be computed.

in contact. This can be done by respecting the following ratio for velocities (combine equations 5 and 8) :

$$\frac{v'}{v} = \frac{a - (L + d)\tan\theta}{a - (L - d)\tan\theta} \qquad (16)$$

In the second mode, the sequence of corridors in which the robot has to navigate between the origin and the goal is given to it. The robot does not follow some pre-defined trajectory, but again uses sensor information and rules of behaviour.

We describe in detail the rule used to perform a turn with no maneuver, when the robot is coming with driving wheels at the front. Before the turn, the robot moves in straight line so that it finally comes to slide with edge $A'B'$ in contact with the vertex of the inner obstacle. The sliding motion goes on until the axis of the wheels gets aligned with the vertex (as wheels are at the front, there is little chance the robot will first bump into edge e^+ of the outer wall). Now the robot starts turning around point H'. Either the turn can be completed this way, or the robot will come into contact with edge e^- at the rear. This means we are now on a γ^- trajectory, and point A must slide on the outer wall. Again this is done by applying equation 16.

The trajectory the robot executes is finally made safe by imposing a velocity-damper type constraint to control the minimum distance with obstacles (as we introduced in [FT87a]), so that it will not hit them.

The following figures illustrate results of the program based on a simulation of the kinematics of the robot and of ultra-sonic sensors. Figure 10 shows how a free mode trajectory is modified to avoid obstacles. The last two figures illustrate the planning algorithm. Figure 11a shows a sequence of cones in which the robot has to navigate, and 11b the resulting trajectory.

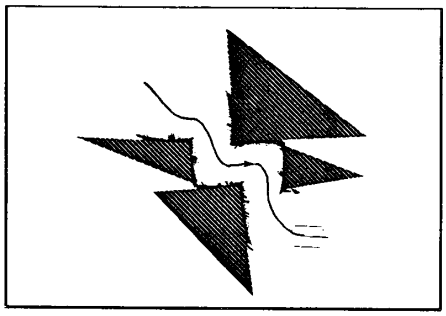

Figure 10: Constrained trajectory (without planning).

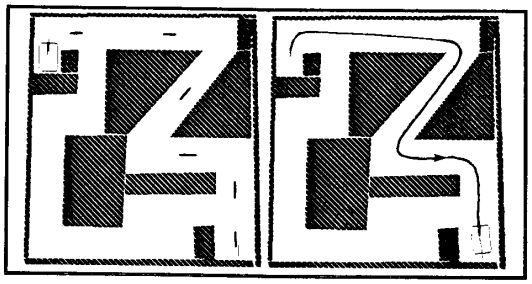

(a) (b)

Figure 11: a) The sequence of cones in which the robot must navigate (only center configurations of the cones are drawn), b) Execution of the corresponding trajectory.

8 Conclusion

We have given in this paper results on the existence of trajectories with no maneuver, or a limited number of maneuvers, for motions of a mobile robot in a corridor with a single turn. Based on these results and a decomposition of free space into cones, a heuristic path planning algorithm has been proposed.

Our approach of implementing those results as a set rules of behaviour for the robot seems promising in many ways. It is realistic as it basically relies on sensor information, yet it permits to incorporate complex maneuvers whose result we know exactly.

Many questions remain open :

- Is it possible to build a reasonably complex exact path-planning algorithm such that we can control the number of maneuvers necessary ?
- What is the computational complexity of finding a shortest length trajectory ?
- What does it become when we impose a higher bound on the number of maneuvers, or when no maneuver at all is allowed ?

Acknowledgments

The authors thank Pierre Janière, Marc Boullé and Eric Iooss for sharing the work of implementing the planning and navigation algorithms. We also thank Bernard Faverjon for his helpful comments.

References

[ABF88] F. Avnaim, J.D. Boissonnat, and B. Faverjon. A practical exact motion planning algorithm for polygonal objects amidst polygonal obstacles. In *Proceedings of IEEE Int. Conference on Robotics and Automation*, 1988.

[BL85] R.A. Brooks and T. Lozano-Pérez. A subdivision algorithm in configuration space for findpath with rotation. In *IEEE Transactions on Systems, Man and Cybernetics, SMC-15(2)*, pages 224–233, 1985.

[Bro82] R.A. Brooks. Solving the find-path problem by representing free space as generalized cones. In *IEEE Transactions on Systems, Man and Cybernetics, SMC-13(2)*, pages 190–197, 1982.

[Fav84] B. Faverjon. Obstacle avoidance using an octree in the configuration space of a manipulator. In *Proceedings of IEEE Int. Conference on Robotics and Automation*, Atlanta, March 1984.

[FT87a] B. Faverjon and P. Tournassoud. A local based approach for path planning of manipulators with a high number of degrees of freedom. In *Proceedings of IEEE Int. Conference on Robotics and Automation*, pages 1152–1159, Raleigh, April 1987. Also INRIA Research Report N 621, February 1987.

[FT87b] B. Faverjon and P. Tournassoud. The mixed approach for motion planning: learning global strategies from a local planner. In *Proceedings of the Int. Joint Conference on Artificial Intelligence*, pages 1131–1137, Milan, August 1987.

[Lau86] J.P. Laumond. Feasible trajectories for mobile robots with kinematic and environment contraints. In *Proceedings of the Int. Conference on Autonomous Systems*, Amsterdam, December 1986.

[Lau87] J.P. Laumond. Finding collision-free smooth trajectories for a non-holonomic mobile robot. In *Proceedings of the Int. Joint Conference on Artificial Intelligence*, pages 1120–1123, Milan, August 1987.

[Loz86] T. Lozano-Pérez. A simple motion planning algorithm for general robot manipulators. In *5th AAAI*, Philadelphia 1986.

[LW79] T. Lozano-Pérez and M. Wesley. An algorithm for planning collision-free paths among polyhedral obstacles. In *Communications of ACM*, pages 560–570, 1979.

[SS83] J.T. Schwartz and M. Sharir. On the piano movers' problem ii: general techniques for computing topological properties of real algebraic manifolds. *Advances in Applied Mathematics*, (4):298–351, 1983.